Title

Heterogeneity of bone microstructure in the femoral head in patients with osteoporosis: An ex vivo HR-pQCT study

Journal

Bone, 56(1)

ISSN

8756-3282

Authors

Chiba, Ko
Burghardt, Andrew J
Osaki, Makoto
et al.

Publication Date

2013-09-01

DOI

10.1016/j.bone.2013.05.019

Peer reviewed

Published in final edited form as:
Bone. 2013 September ; 56(1): 139–146. doi:10.1016/j.bone.2013.05.019.

Heterogeneity of Bone Microstructure in the Femoral Head in Patients with Osteoporosis: an *ex vivo* HR-pQCT study

Ko Chiba[1,2], **Andrew J. Burghardt**[1], **Makoto Osaki**[2], and **Sharmila Majumdar**[1]

[1]Musculoskeletal Quantitative Imaging Research Group, Department of Radiology and Biomedical Imaging, University of California, San Francisco; San Francisco, CA USA

[2]Department of Orthopedic Surgery, Nagasaki University School of Medicine; Nagasaki, Japan

Abstract

Introduction—Trabecular bone in the femoral head has a complicated and heterogeneous structure with few studies having analyzed heterogeneity in this structure quantitatively. We analyze trabecular bone microstructure in the femoral head with osteoporosis (OP) using high resolution peripheral quantitative CT (HR-pQCT) to investigate its regional characteristics.

Methods—Fifteen femoral heads extracted from female OP patients with femoral neck fracture (85 ± 7, 67–94 years) were scanned by HR- pQCT at 41 μm voxel size. The femoral head was segmented into 15 regions (3 longitudinal regions: superior, center, and inferior, and 5 axial subregions: center, medial, lateral, anterior, posterior). Of these 15 regions, five were excluded due to overlap with the fracture site, leaving a total of 10 regions of cancellous bone microstructures to be quantitatively assessed using the following parameters: bone volume fraction, trabecular thickness, number, separation, connectivity density, structure model index, and degree and orientation of anisotropy. These parameters were compared among each region.

Results—Trabecular bone at the center, superior, and supero-posterior regions of the femoral head had higher bone volume, trabecular number, thickness, narrower bone marrow spaces, higher connectivity and anisotropy, and more plate-like structure. This plate-like structure ran supero-inferiorly and antero-posteriorly at the superior and center regions. Bone volume at the anterior, posterior, and medial regions was almost half of the central and superior regions.

Conclusion—Significant heterogeneity of the trabecular bone microstructure in the OP femoral head was showed quantitatively in this study. These data offer new insight into bone microstructural anatomy and may prove to provide useful information on clinical medicine such as hip surgeries.

Keywords

HR-pQCT; Osteoporosis; Femoral Head; Bone Microstructure; Femoral Neck Fracture

Corresponding author: Ko Chiba, Musculoskeletal Quantitative Imaging Research Group, Department of Radiology and Biomedical Imaging, University of California, San Francisco, 1700 4th Street, QB3 Building, Suite 203, San Francisco, CA 94158, Tel: +1 (415) 514-9658, Fax: +1 (415) 514-9656, kohchiba@estate.ocn.ne.jp.

Conflicts of Interest
None.

Introduction

Osteoporosis (OP) is one of the most common diseases in elderly people, with OP fractures in this population playing a significant role in the reduction in activity of daily living (ADL). In particular, patients with OP fractures at the proximal femur require surgery and a long recovery process to resume normal activity with a decrease in their vital prognosis. (1,2)

The proximal femur has a unique morphology, with the trabecular bone having a complicated and heterogeneous structure. Bone microstructure analysis has played an important role in OP research. However, most of the previous studies regarding bone microstructure in the OP proximal femur have only been performed on bone specimens using micro CT. (3–6) In these studies, small bone samples were extracted from bone specimens and their microstructure was analyzed. The whole bone microstructure in the OP proximal femur is still not well-characterized.

High Resolution peripheral Quantitative CT (HR-pQCT) can image human peripheral skeletal sites such as the distal radius and distal tibia at high resolution with a voxel size of 82 μm, thus enabling *in vivo* bone microstructure analysis. (7,8) HR-pQCT is also useful for *ex vivo* bone microstructure analysis for larger bone specimens. (9–11) Bone specimens up to 12.6 cm in diameter and 15 cm in length can be scanned at a higher resolution with a voxel size of 41 μm, allowing trabecular bone microstructure to be analyzed (Fig. 1).

Analyzing the microstructure in the OP femoral head may help obtain new information that could prove to be clinically significant. For example, investigating regional features of bone microstructure would provide more detail about the anatomy of the femoral head, which would be useful information for surgical interventions such as osteosynthesis and osteotomy. Moreover, cross-sectional analysis of the correlation between bone volume and bone microstructure may provide insight into bone microstructural changes due to OP development, and allow us to gain a better understanding of OP pathophysiology.

We analyzed bone microstructure in the femoral head extracted from patients with OP using HR-pQCT with the following research questions in mind: (1) What are the features of bone microstructure in each region of the OP femoral head, and (2) what is the correlation between bone mass and bone microstructure in each region.

Methods

Materials

Fifteen Japanese OP patients with femoral neck fracture who had undergone femoral head replacement at Nagasaki Yurino hospital and Nishi-Isahaya hospital participated in this study (mean age 85 ± 7 years, range 67–94 years, all female). Males, as well as patients who had any sign of bone and joint diseases such as osteoarthritis and rheumatoid arthritis, or who took medicines affecting bone metabolism were excluded from the study. The mean height was 145 ± 9 cm (130–160 cm), weight was 44.1 ± 6.3 kg (35.0–52.0 kg), and BMI was 21.0 ± 3.0 kg/m^2 (17.6–25.0). Fifteen femoral head specimens were obtained during surgery and stored in a freezer. The study protocol was approved by the ethics review board of our institute and complied with the Declaration of Helsinki of 1975, revised in 2000.

Imaging

Bone specimens were thawed gradually, put on the dedicated device with the posterior site of the femoral head facing the CT gantry table, and fastened with Velcro. They were then scanned by HR-pQCT (XtremeCT, Scanco Medical, Brüttisellen, Switzerland) with a voxel size of 41 μm using the following scan settings: x-ray tube voltage 60 kVp, tube current 900

μAs, field of view 126 mm, matrix size 3072×3072, exposure time 300 ms, and number of projections 1000. The spatial resolution was 88 μm. (12) Scan length was approximately 44 mm, resulting in 1070 slices and a 37 minute scan time.

Measurements

Using bone microstructure measurement software (TRI/3D-BON, Ratoc System Engineering, Japan), adjustment of the femoral head orientation, segmentation of the regions of interest (ROI), and measurement of bone microstructural parameters in each region were performed.

Orientations of all femoral heads were adjusted based on anatomical landmarks using the principal compressive trabeculae and fovea capitis femoris (Fig. 2 A–C). In the multi-planar reconstructed images, the femoral heads were rotated so the principal compressive trabeculae were oriented along the supero-inferior axis in coronal and sagittal views, and the fovea capitis femoris faced medially in the axial view.

The femoral head was divided into 15 regions (Fig. 2 A–C). In coronal and sagittal views, the femoral head was divided into 3 equal regions (superior, center, and inferior). Then in axial views, each region was subdivided into 5 sub-regions (center, medial, lateral, anterior, posterior) by setting a square, with side lengths equal to 1/3 of the femoral head maximum diameter, in the center and drawing 4 lines outward from the vertex.

A fixed threshold value was used for the binarization of the bone images in this study. From the histogram of the cancellous bone region in 5 arbitrary specimens, the threshold between bone and background was determined by discriminant analysis. Their mean threshold value (340 mg/cm^3) was used as the fixed threshold for the analysis of all specimens.

By filling bone marrow spaces in the binarized bone images, the entire bone region was obtained. Then, by deleting the cortical shell (subchondral bone plate), the cancellous bone region was extracted (Fig. 2 D). Based on the thickness of the cortical shell in the femoral head ranging from approximately 100 to 700 μm, the cortical shell region was excluded automatically by eroding the entire bone region 1 mm from the surface.

After manual deletion of the remaining bone fragments on the surface of the fracture line, a contour containing the cancellous bone area was obtained automatically. By removing the contour under the intact cortical shell, the fracture line was identified. Regions within a 2.5 mm margin from fracture line were automatically excluded from the measurement regions (Fig. 2 D). Regions that consistently lost more than 1/2 of their volume were excluded from further analysis. As a result, 5 common fracture regions (Cen-Lat, Inf-Cen, Inf -Lat, Inf -Ant, Inf -Post) were not studied further. Thus, a total of 10 regions (Sup-Cen, Sup-Med, Sup-Lat, Sup-Ant, Sup-Post, Cen-Cen, Cen-Med, Cen-Ant, Cen-Post, and Inf-Med), where the bone volume was intact, were included in the statistical analysis (Fig. 2 E). One Cen-Pos region and three Inf-Med regions from a total of 15 subjects were excluded from their respective group because the fracture extended to these regions for these unusual cases (Table 1).

The following trabecular bone microstructure parameters were measured in each ROI: bone volume fraction (BV/TV) (%), trabecular thickness (Tb.Th) (μm), trabecular number (Tb.N) (1/mm), trabecular separation (Tb.Sp) (μm), connectivity density (ConnD) (1/mm^3), structure model index (SMI), degree of anisotropy (DA), and orientation of anisotropy (MIL axes: a-theta, a-phi, b-theta, and b-phi). (13)

ConnD is a parameter of trabecular connectivity, where a higher value indicates greater connectivity. (14) SMI is an index evaluating whether trabecular bone is rod-like or plate-like; with 0 indicating a plate-like structure and 3 indicating a rod-like structure. (15)

DA and orientation of anisotropy were calculated by the mean intercept length (MIL) method. (16) DA is determined by the ratio between the primary and tertiary axes of the MIL ellipsoid (DA=a/c), with a higher value indicating higher anisotropy (Fig. 3 A).

Orientation of anisotropy is expressed by the orientation of the MIL primary axis in coordinate space, which is defined as the angles between the MIL primary axis, and the z and y axes (a-theta and a-phi) (Fig. 3 B). In this study, these angles were transformed into the absolute value to draw focus on how much the trabecular bone ran along the direction of the z (superio-inferior), y (antero-posterior), or x (medio-lateral) axes. For example, |a-theta| =0 indicates the trabecular bone ran superio-inferiorly, |a-theta|=90 and |a-phi|=0 means the trabecular bone ran antero-posteriorly, and |a-theta|=90 and |a-phi|=90 means the trabecular bone ran medio-laterally. In instances where |a-theta| is around 45 and |a-phi|=0, the original data was further examined to determine whether the trabecular bone ran from supero-anterior to infero-posterior, or supero-posterior to infero-anterior.

In the plate-like structure, the orientation of the MIL secondary axis also has structural importance. For example, |a-theta|=0, |b-theta|=90, and |b-phi|=0 means the plate-like trabeculae run superio-inferiorly and antero-posteriorly. |a-theta|=0, |b-theta|=90, and |b-phi| =90 means the plate-like trabeculae run superio-inferiorly and medio-laterally.

Statistical analysis

Statistical analysis was performed using SPSS ver.16.0 (SPSS, Chicago, IL, USA). Microstructural parameters were compared among each region by ANOVA with a Bonferonni correction to account for multiple comparisons. The correlations between BV/TV and the other microstructural parameters were analyzed by Pearson's correlation coefficient. For all analyses, the level of statistical significance was established at $P < 0.01$.

Results

Regional Characteristics of Bone Microstructure

Metric parameters for bone microstructure in each region are presented in Table 1. Significant regional differences were observed in all parameters, most notably in BV/TV and Tb.N. BV/TV was significantly higher in Cen-Cen, Sup-Cen, and Sup-Pos regions, and lower in Sup-Med, Cen-Med, and Inf-Med regions (average 24.2, 21.0, 17.9, 9.8, 8.0, and 6.2 %, respectively, $P<0.01$). This is also shown as a bar graph in Fig. 4. The same tendency was seen in Tb.N (average 0.676, 0.669, 0.628, 0.351, 0.326, and 0.245 mm, respectively, $P<0.01$). Tb.Th was significantly the highest in the Cen-Cen region (average 261 um, $P<0.01$). Tb.Sp was higher in the Inf-Med region, and lower in the Cen-Cen and Sup-Pos region (average 980, 667, and 665 um, respectively, $P<0.01$).

Table 2 shows non-metric bone microstructure parameters in each region. Conn.D was significantly higher in Cen-Cen, Sup-Cen, and Sup-Pos regions, and lower in Sup-Med, Cen-Med, and Inf-Med regions (average 1.82, 1.86, 2.05, 0.73, 0.75, and 0.43 mm, respectively, $P<0.01$). The same tendency was seen in DA (average 2.34, 2.36, 1.96, 1.64, 1.31, and 1.48, respectively, $P<0.01$), which means trabecular bone has higher connectivity and anisotropy in Cen-Cen, Sup-Cen, and Sup-Pos regions. SMI was significantly lower in Cen-Cen, Sup-Cen, and Sup-Pos regions, and higher in Sup-Med, Cen-Med, and Inf-Med regions (average 1.33, 1.59, 1.94, 2.57, 2.54, and 2.63, respectively, $P<0.01$), which means

the trabeculae were moderately plate-like in Cen-Cen, Sup-Cen, and Sup-Pos regions, and highly rod-like in the medial regions.

Orientations of the MIL primary axis (|a-theta| and |a-phi|) and secondary axis (|b-theta| and |b-phi|) represent orientations of trabecular anisotropy and plate-like structure, respectively (Fig.3). Therefore, these parameters only have a specific meaning in regions where DA is significantly higher and SMI is lower (Sup-Cen, Cen-Cen, and Sup-Pos region). In Sup-Cen and Cen-Cen regions, |a-theta| was close to 0°, |b-theta| was close to 90°, and |b-phi| was close to 0°, which means that the MIL primary axis ran along the z-axis (supero-inferiorly) and the secondary axis ran along the y-axis (antero-posteriorly). The 3D images of trabecular bone at the Sup-Cen region are demonstrated in Fig.5. In the Sup-Pos region, |a-theta| was 33°, |a-phi| was close to 0°, |b-theta| was 58°, and |b-phi| was close to 0°, indicating the MIL primary axis ran at a 33° angle with the z-axis from the supero-posterior to infero-anterior direction in the y-z plane and the secondary axis ran with a 58° angle with the z-axis from supero-anterior to infero-posterior in the y-z plane.

Correlation between Bone Volume and Bone Microstructure

Table 3 shows the correlation between BV/TV and other bone microstructure parameters in each region. A positive correlation was found between BV/TV and Tb.Th, Tb.N, and Conn.D, and negative correlation between BV/TV and Tb.Sp and SMI in almost all regions (|R| ranging from 0.69 to 0.98, $P<0.01$). BV/TV was negatively correlated with DA in Cen-Cen, Sup-Ant, Sup-Cen, and Sup-Pos regions (R ranging from −0.64 to −0.80, $P<0.01$). As shown in Fig. 6, patients with lower BV/TV had thinner Tb.Th, lower Tb.N, wider Tb.Sp, lower Conn.D, higher SMI (more rod-like), and higher DA.

Discussion

As far as we know, this is the first study analyzing regional characteristics of bone microstructure in the femoral head in patients with osteoporotic hip fractures. Most of the previous studies have analyzed bone microstructure in a part of the femoral head using micro CT, HR-pQCT, clinical CT, and MRI. (3–5,9,17–18)

The heterogeneity of bone microstructure in the femoral head as showed in Table 1, 2, and Figure 4 might be caused by a heterogeneous load distribution in the hip joint and the proximal femur as previous reports have shown. The femoral head articulates with the acetabulum across its superior and posterior surfaces, with the medial side facing the acetabular fossa and the femoral head ligament, and the lateral side facing the joint capsule and the gluteus minimus muscle. Therefore, higher weight bearing across the superior and posterior surface of the hip joint would be expected to produce higher bone volume, trabecular number, thickness, connectivity, anisotropy, and a plate-like structure at the superior, supero-posterior, and central regions (Sup-Cen, Sup-Pos, and Cen-Cen) of the femoral head, spanning the principal path for load transfer from the femoral head to the femoral diaphysis. In contrast, lower weight bearing over the medial surface would be expected to be associated with lower bone volume, trabecular number, connectivity, anisotropy, and rod-like structure at medial regions (Sup-Med, Cen-Med, and Inf-Med).

Load distribution in the hip joint might also influence the orientation of anisotropy, resulting in trabecular bone running supero-inferiorly in the superior and central regions (Sup-Cen and Cen-Cen), and from the supero-posterior to infero-anterior direction in the supero-posterior region (Sup-Pos) (Table 2).

Plate-like structures running supero-inferiorly (MIL primary axis) and antero-posteriorly (MIL secondary axis) at the superior and center (Sup-Cen and Cen-Cen) regions might be

caused by loading patterns in the hip joint (Fig. 5). Habitual movement of the hip joint primarily consists of hip flexion-extension (e.g. walking, running, standing up, sitting down, and walking up/down stairs). This loading pattern in the sagittal plane may be related to the plate-like bone formation in the femoral head.

Bone microstructure in the femoral head is regulated by load distribution in not only the hip joint but also the proximal femur. Trabecular bones in the proximal femur have been studied by anatomic sections and macro radiographs, and their distribution has been classified into five groups: the principal compressive group, the principal tensile group, the secondary compressive group, the secondary tensile group, and the greater trochanter group. (19–21) Those trabecular groups are distributed heterogeneously but adjusted properly to the load distribution in the proximal femur according to Wolf's law. (22) The principal compressive group runs from the superior aspect of the femoral head to the medial cortex of the femoral neck, and is preserved preferentially while OP develops. The principal tensile group runs from the medial region of the femoral head to the greater trochanter, intersecting with the principal compressive group at the center of the femoral head. Those trabecular groups also explain the bone microstructural features we observed by HR-pQCT.

These findings have potentially important implications for optimal screw positioning for orthopedic procedures including osteosynthesis for hip fracture, and osteotomy for hip deformity and osteoarthritis. Previously, the center of the femoral head has been considered the ideal position for screw placement, with inaccurate screw insertion into the anterior region of the femoral head increasing the risk for screw cut-out. (23,24) Our data supports these conclusions, most notably in the BV/TV distribution throughout the femoral head with the most central region (Cen-Cen region) being of highest value. Inaccurate screw insertions occur occasionally due to poor lateral x-ray images in the operating room. If the screw is inserted into the anterior or posterior parts of the femoral head (Cen-Ant and Cen-Pos regions), where the BV/TV is almost half of the central part (Cen-Cen region), there may be an increased risk for screw failure and the need for further corrective surgery (Table 1, Fig. 4). In the case of the medial region (Cen-Med), where the BV/TV is almost 1/3 of the central region, screw insertion would be less likely to cause serious problems as the screw would be likely achieve partial anchorage in the dense central region.

Individual differences of bone microstructure in the femoral head were also found across the specimens studied here. In the case of BV/TV shown in table 1, the range of values across subjects spanned more than ± 50% of the mean, indicating some patients had highly fragile bone microstructure even in high bone volume regions such as the central region. This would be another issue to consider when evaluating patients for hip surgery.

As expected, lower bone volume was associated with smaller and fewer trabeculae, wider bone marrow spaces, less trabecular connectivity, a more rod-like structure, and higher anisotropy in almost all regions (Table 3, Fig. 6). Higher anisotropy might be caused by selective bone loss in the process of OP development. Trabeculae perpendicular to the loading direction may decrease disproportionately, while trabeculae parallel to the loading direction are preserved, resulting in increased anisotropy.

Previously, osteoporotic changes of trabecular bone in the femoral head have been semi-quantitatively evaluated by plain radiographs. Based on changes in the principal compressive and tensile trabecular bones observed from an anterior-posterior view, the degree of osteoporosis has been typically classified into six grades based on severity (Singh Index). (21) As OP develops, bone is primarily lost in the principal tensile group, which runs laterally from the femoral head to the greater trochanter, and subsequently bone loss occurs

in the principal compressive group. This might explain why the degree of anisotropy increases with OP progression in our study.

Clinical CT has enabled us to three-dimensionally evaluate quantitative parameters such as bone mineral density, but this technology currently lacks the resolution needed to accurately quantify trabecular bone microstructure. (25–26)

Stauber and Müller used micro CT to investigate age-related changes in trabecular bone microstructure at 4 mm cube regions of cancellous bone samples extracted from the femoral heads and lumber spine of human cadavers. (3) Cui et al also performed micro CT scan on 8 mm diameter cancellous bone extracted from the femoral head, neck, and trochanter of male cadavers to analyze age-related changes and found that with regards to the femoral head, BV/TV, Tb.Th and Tb.N decreased, and Tb.Sp increased with aging. (4) Zhang et al analyzed 5 mm diameter and 10 mm high cancellous bone cores extracted from the femoral heads of osteoarthritis and OP patients using micro CT, and reported that OP patients showed smaller BV/TV and Tb.N, and greater SMI (more rod-like structure). (5) These results support the findings of bone microstructural changes due to bone loss in our study.

Our study has some limitations. Fractured regions were excluded from the analysis because the bone microstructure was destroyed making the regions unquantifiable. In addition, we did not analyze regions where osteoporotic fractures are typically found, such as the femoral neck and trochanter. This means our study did not contribute to the understanding of the pathogenesis of these types of fractures. Moreover, we did not analyze cortical bone structure and bone mineral density. This study was primarily concerned with the cancellous bone microstructure of the femoral head, including its heterogeneity and associated osteoporotic changes. Studies using cadavers with OP would be able to investigate a larger area of bone microstructure in the proximal femur. Hansen et al studied bone microstructure of the femoral head, neck, greater trochanter, and lessor trochanter using femur specimens by HR-pQCT and compared them with compressive strength obtained by biomechanical testing. This group scanned a 9.02 mm width center cross section of the femoral head, and found higher BV/TV and Tb.N values in the femoral head than seen in the femoral neck and trochanter. (9)

The number of subjects was not large in this study (N=15) and therefore further studies with a larger sample size would be needed to validate our results. Originally, we collected bone specimens from 33 femoral heads, but after initial scanning 18 of them had to be excluded because they had bony damages due to the operation. All of these bone specimens were derived from OP patients with femoral neck fractures, and we did not have healthy controls in this study. So, we were not able to reveal if the degree of microstructural heterogeneity in the femoral head was specific for OP patients or even healthy controls have the same tendency. This was a cross-sectional study using femoral head specimens, and our assumptions on osteoporotic changes were based on this cross-sectional data. It is impossible to perform HR-pQCT scanning on hip joints *in vivo*. Future development and increased spatial resolution in clinical CT and MRI would help solve this problem. (**17, 18, 27, 28**)

Orientation of the femoral heads were adjusted by the principal compressive trabeculae and fovea capitis femoris, but the directions of these anatomical landmarks may vary slightly across subjects as a result of natural morphological differences and the positioning of the limb. Generally, the orientation of the principal compressive trabeculae is such that it declines medially (10~30 degree) and anteriorly from the plumb line, which in turn depends on the femoral neck shaft angle and femoral anteversion. The fovea capitis femoris faces

medially, but may vary according to hip internal and external rotation (toe-in and toe-out gait).

In conclusion, this study demonstrated the central, superior, and supero-posterior regions of the femoral head had higher bone volume, trabecular number, connectivity, anisotropy, and plate-like structure compared to the rest of the femoral head. These plate-like structures run supero-inferiorly and antero-posteriorly at the superior and center of the femoral head. This heterogeneous bone microstructure in the femoral head would be caused by heterogeneous load distribution in the hip joint and the proximal femur.

The maximum difference of bone volume between individuals was more than two times. Lower bone volume was related to less trabecular thickness, number, and connectivity, wider bone marrow spaces, more rod-like structure, and higher anisotropy.

These quantitative data indicating regional and individual heterogeneities of the trabecular bone microstructure in the OP femoral head provide new insight into bone microstructural anatomy and may prove to be useful information on clinical medicine such as hip surgeries.

Acknowledgments

The authors would like to thank Ryoichi Takasuga (Department of Orthopedic Surgery, Nagasaki Yurino Hospital, Nagasaki, Japan) and Goji Chiba (Department of Orthopedic Surgery, Nishi-Isahaya Hospital, Nagasaki, Japan) for collecting the bone specimens. This research was supported by NIH R01 AG17762 (SM).

References

1. Alarcón T, González-Montalvo JI, Gotor P, Madero R, Otero A. Activities of daily living after hip fracture: profile and rate of recovery during 2 years of follow-up. Osteoporos Int. 2010; 22:1609–1613. [PubMed: 20521027]
2. Vestergaard P, Rejnmark L, Mosekilde L. Increased mortality in patients with a hip fracture-effect of pre-morbid conditions and post-fracture complications. Osteoporos Int. 2007; 18:1583–1593. [PubMed: 17566814]
3. Stauber M, Müller R. Age-related changes in trabecular bone microstructures: global and local morphometry. Osteoporosis International. 2006; 17:616–626. [PubMed: 16437194]
4. Cui WQ, Won YY, Baek MH, Lee DH, Chung YS, Hur JH, Ma YZ. Age-and region-dependent changes in three-dimensional microstructural properties of proximal femoral trabeculae. Osteoporosis International. 2008; 19:1579–1587. [PubMed: 18437273]
5. Zhang ZM, Li ZC, Jiang LS, Jiang SD, Dai LY. Micro-CT and mechanical evaluation of subchondral trabecular bone structure between postmenopausal women with osteoarthritis and osteoporosis. Osteoporosis International. 2010; 21:1383–1390. [PubMed: 19771488]
6. Milovanovic P, Djonic D, Marshall RP, Hahn M, Nikolic S, Zivkovic V, Amling M, Djuric M. Micro-structural basis for particular vulnerability of the superolateral neck trabecular bone in the postmenopausal women with hip fractures. Bone. 2012; 50:63–68. [PubMed: 21964412]
7. Burghardt AJ, Link TM, Majumdar S. High-resolution Computed Tomography for Clinical Imaging of Bone Microarchitecture. Clinical orthopaedics and related research. 2011; 469:2179–2193. [PubMed: 21344275]
8. Patsch JM, Burghardt AJ, Kazakia G, Majumdar S. Noninvasive imaging of bone microarchitecture. Annals of the New York Academy of Sciences. 2011; 1240:77–87. [PubMed: 22172043]
9. Hansen S, Jensen J-EB, Ahrberg F, Hauge EM, Brixen K. The Combination of Structural Parameters and Areal Bone Mineral Density Improves Relation to Proximal Femur Strength: An In Vitro Study with High-Resolution Peripheral Quantitative Computed Tomography. Calcified Tissue International. 2011; 89:335–346. [PubMed: 21874544]
10. Wang Y, Boyd SK, Battié MC, Yasui Y, Videman T. Is greater lumbar vertebral BMD associated with more disk degeneration? A study using μCT and discography. Journal of Bone and Mineral Research. 2011; 26:2785–2791. [PubMed: 21786320]

11. Mueller TL, Christen D, Sandercott S, Boyd SK, Van Rietbergen B, Eckstein F, Lochmüller E-M, Müller R, van Lenthe GH. Computational finite element bone mechanics accurately predicts mechanical competence in the human radius of an elderly population. Bone. 2011; 48:1232–1238. [PubMed: 21376150]
12. Tjong W, Kazakia GJ, Burghardt AJ, Majumdar S. The effect of voxel size on high-resolution peripheral computed tomography measurements of trabecular and cortical bone microstructure. Medical physics. 2012; 39:1893–1903. [PubMed: 22482611]
13. Hildebrand T, Rüegsegger P. A new method for the model-independent assessment of thickness in three-dimensional images. Journal of microscopy. 1997; 185:67–75.
14. Odgaard A, Gundersen HJ. Quantification of connectivity in cancellous bone, with special emphasis on 3-D reconstructions. Bone. 1993; 14:173–182. [PubMed: 8334036]
15. Hildebrand TOR, Rüegsegger P. Quantification of Bone Microarchitecture with the Structure Model Index. Computer methods in biomechanics and biomedical engineering. 1997; 1:15–23. [PubMed: 11264794]
16. Whitehouse WJ. The quantitative morphology of anisotropic trabecular bone. Journal of microscopy. 1974; 101:153–168. [PubMed: 4610138]
17. Baum T, Carballido-Gamio J, Huber MB, Müller D, Monetti R, Räth C, Eckstein F, Lochmüller EM, Majumdar S, Rummeny EJ, Link TM, Bauer JS. Automated 3D trabecular bone structure analysis of the proximal femur--prediction of biomechanical strength by CT and DXA. Osteoporosis International. 2010; 21:1553–1564. [PubMed: 19859642]
18. Krug R, Banerjee S, Han ET, Newitt DC, Link TM, Majumdar S. Feasibility of in vivo structural analysis of high-resolution magnetic resonance images of the proximal femur. Osteoporosis International. 2005; 16:1307–1314. [PubMed: 15999292]
19. Meyer GH. Archief fur den anatomische und physiologischen Wissenschaften im Medizin. Die Architektur der Spongiosa. 1867:615–628.
20. Culmann, K. Die Graphische Statik. Zurich, Switzerland: Verlag von Meyer & Zeller; 1866.
21. Singh M, Nagrath AR, Maini PS. Changes in trabecular pattern of the upper end of the femur as an index of osteoporosis. The Journal of bone and joint surgery American volume. 1970; 52:457–467. [PubMed: 5425640]
22. Wolff, J. Berlin, Germany: Verlag von August Hirschwald; 1892. Das Gesetz der Transformation der Knochen.
23. Den Hartog BD, Bartal E, Cooke F. Treatment of the unstable intertrochanteric fracture. Effect of the placement of the screw, its angle of insertion, and osteotomy. The Journal of bone and joint surgery American volume. 1991; 73:726–733. [PubMed: 2045397]
24. Güven M, Yavuz U, Kadıoğlu B, Akman B, Kılınçoğlu V, Ünay K, Altıntaş F. Importance of screw position in intertrochanteric femoral fractures treated by dynamic hip screw. Orthopaedics & Traumatology: Surgery & Research. 2010; 96:21–27.
25. Cody DD, Divine GW, Nahigian K, Kleerekoper M. Bone density distribution and gender dominate femoral neck fracture risk predictors. Skeletal radiology. 2000; 29:151–161. [PubMed: 10794552]
26. Huber MB, Carballido-Gamio J, Bauer JS, Baum T, Eckstein F, Lochmüller EM, Majumdar S, Link TM. Proximal femur specimens: automated 3D trabecular bone mineral density analysis at multidetector CT--correlation with biomechanical strength measurement. Radiology. 2008; 247:472–481. [PubMed: 18430879]
27. Chiba K, Ito M, Osaki M, Uetani M, Shindo H. In vivo structural analysis of subchondral trabecular bone in osteoarthritis of the hip using multi-detector row CT. Osteoarthritis and cartilage / OARS, Osteoarthritis Research Society. 2011; 19:180–185.
28. Mulder L, Van Rietbergen B, Noordhoek NJ, Ito K. Determination of vertebral and femoral trabecular morphology and stiffness using a flat-panel C-arm-based CT approach. Bone. 2012; 50:200–208. [PubMed: 22057082]

Highlights

- Trabecular bone microstructure of the femoral head with osteoporosis was analyzed using HR-pQCT.
- Extremely heterogeneous bone microstructure was observed in the femoral head.
- Higher bone volume, trabecular number, connectivity, anisotropy, and plate-like structure were observed at the center, superior, and supero-posterior regions.

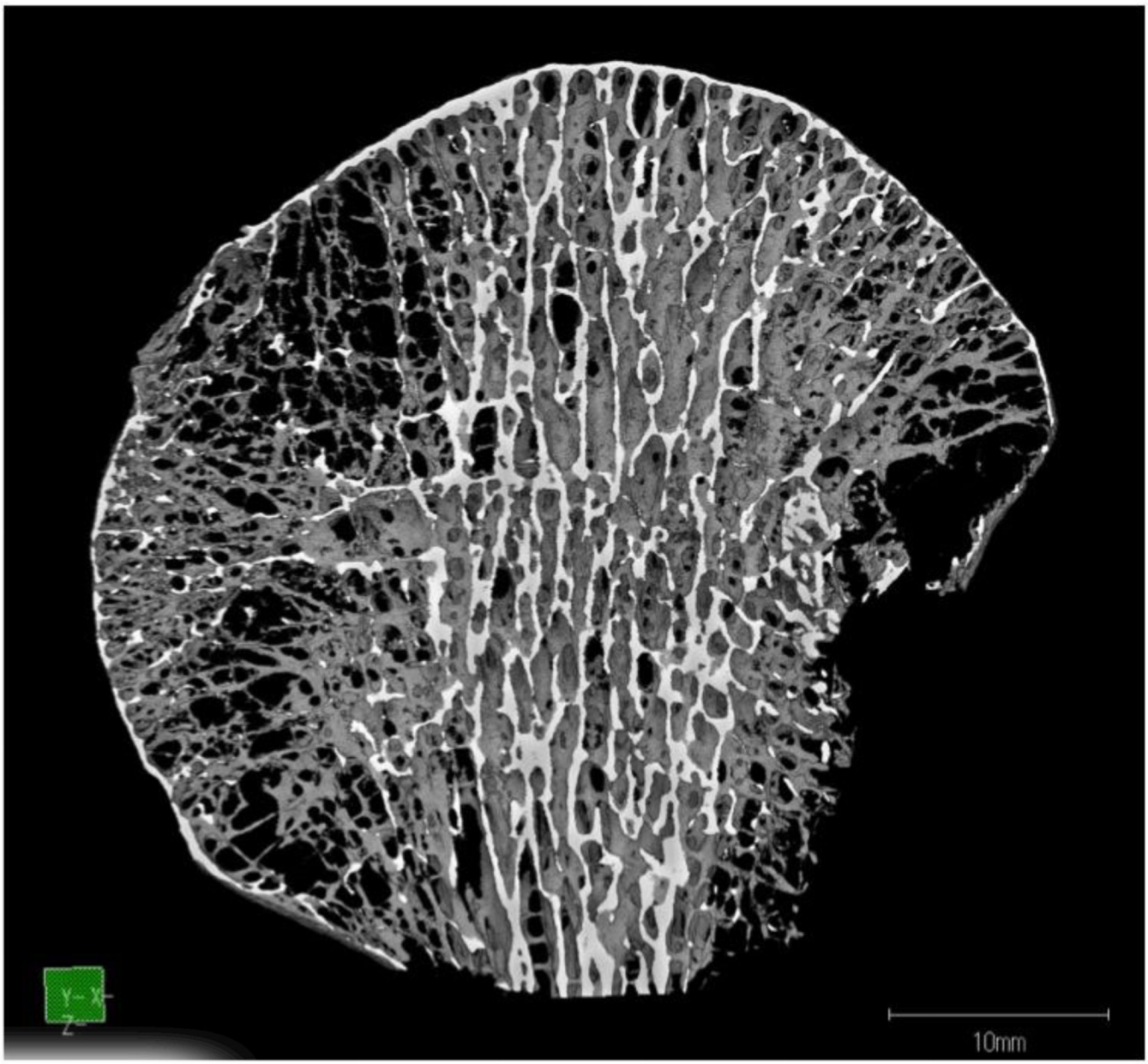

Fig. 1.
3D image of the femoral head of 76 y.o. female patient with femoral neck fracture. Ex vivo HR-pQCT allows high resolution images (pixel size 41 um, isotropic) of large bone specimens (within 126 mm in diameter, 150 mm length) to be obtained.

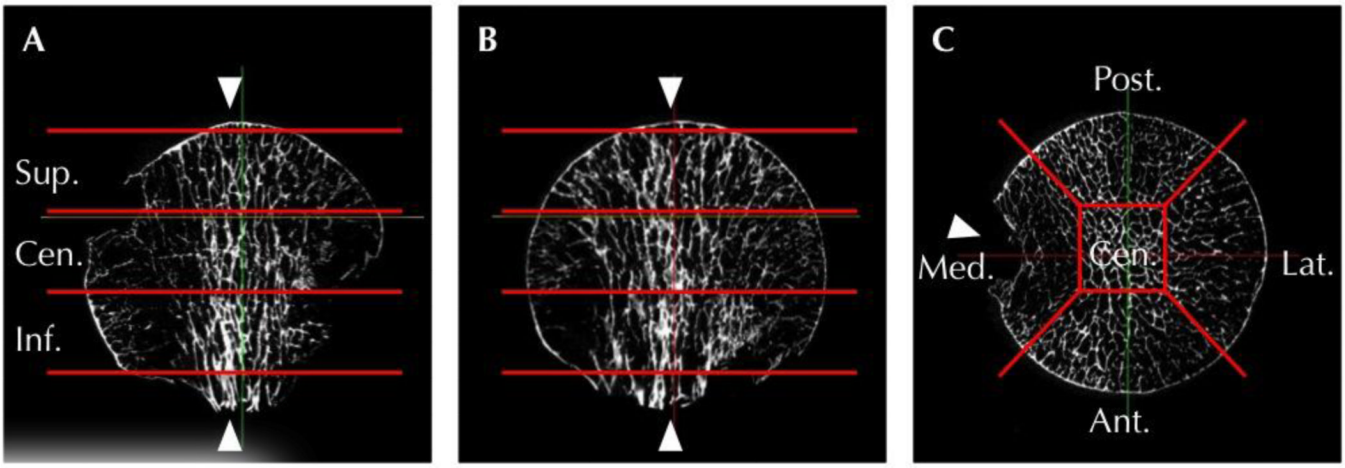

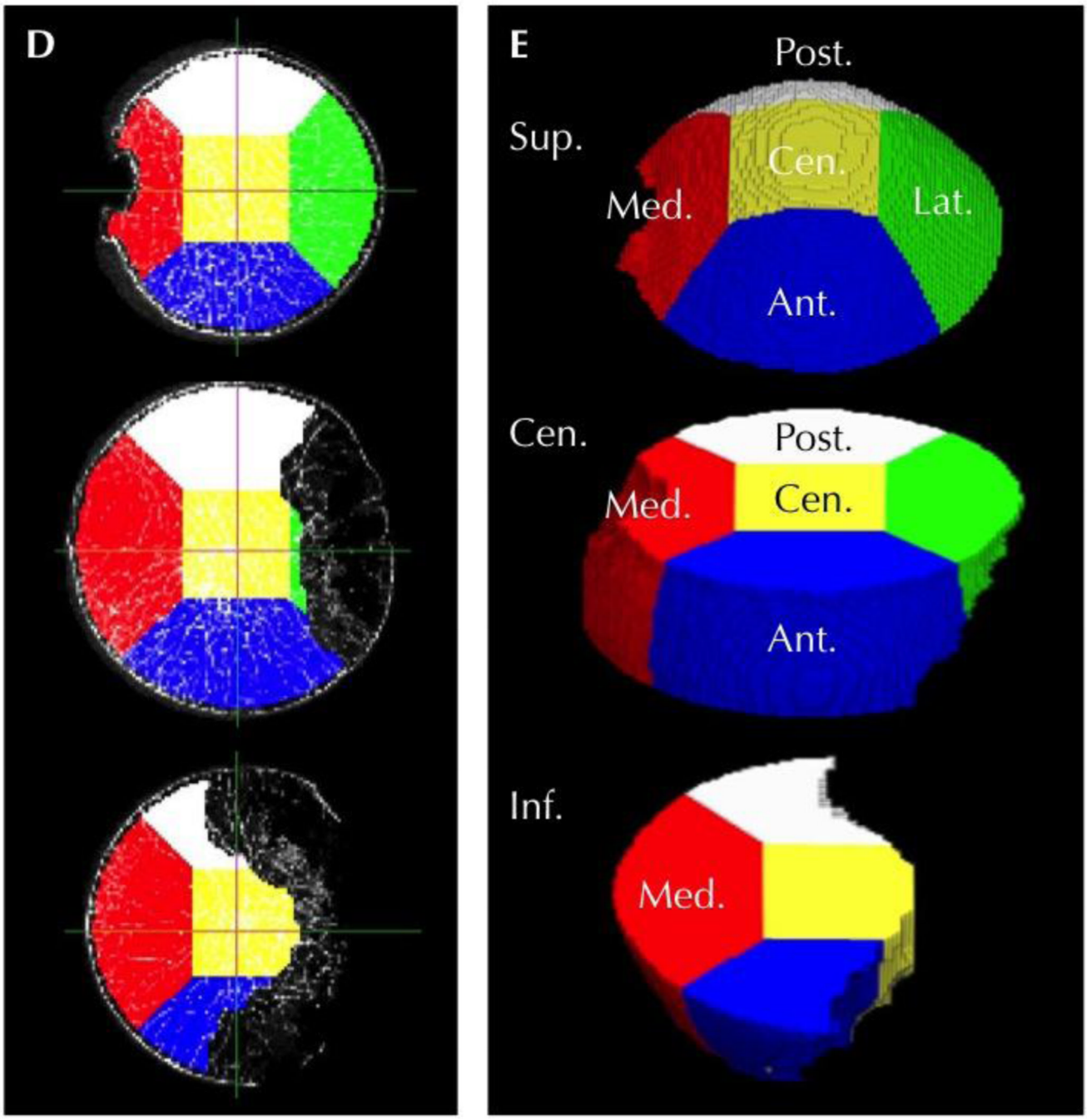

Fig. 2.

A–C, Multi-planar reconstructed images of the femoral head (A–C). Orientations of all femoral head specimens were adjusted by anatomical landmarks: lining up the principal compressive trabecular band (arrows) supero-inferiorly in the coronal and sagittal views (A, B), and facing the fovea capitis femoris (arrow) medially in the axial view (C). The femoral head was divided into 3 regions (Sup., Cen., and Inf.) (A, B), and then each region was sub-divided into 5 regions (Cen., Med., Lat., Ant., and Post.) (C).

D–E, Overlaid images of CT axial view and ROIs (D) and 3D images of ROIs (E). Fracture regions were excluded with a 2.5 mm margin (D). As a result, 5 regions (Cen-Lat, Inf-Cen, Inf -Lat, Inf -Ant, Inf -Post) were not ultimately studied. Cancellous bone microstructure

was measured in the 10 remaining regions (Sup-Cen, Sup-Med, Sup-Lat, Sup-Ant, Sup-Post, Cen-Cen, Cen-Med, Cen-Ant, Cen-Post, and Inf-Med) (E).

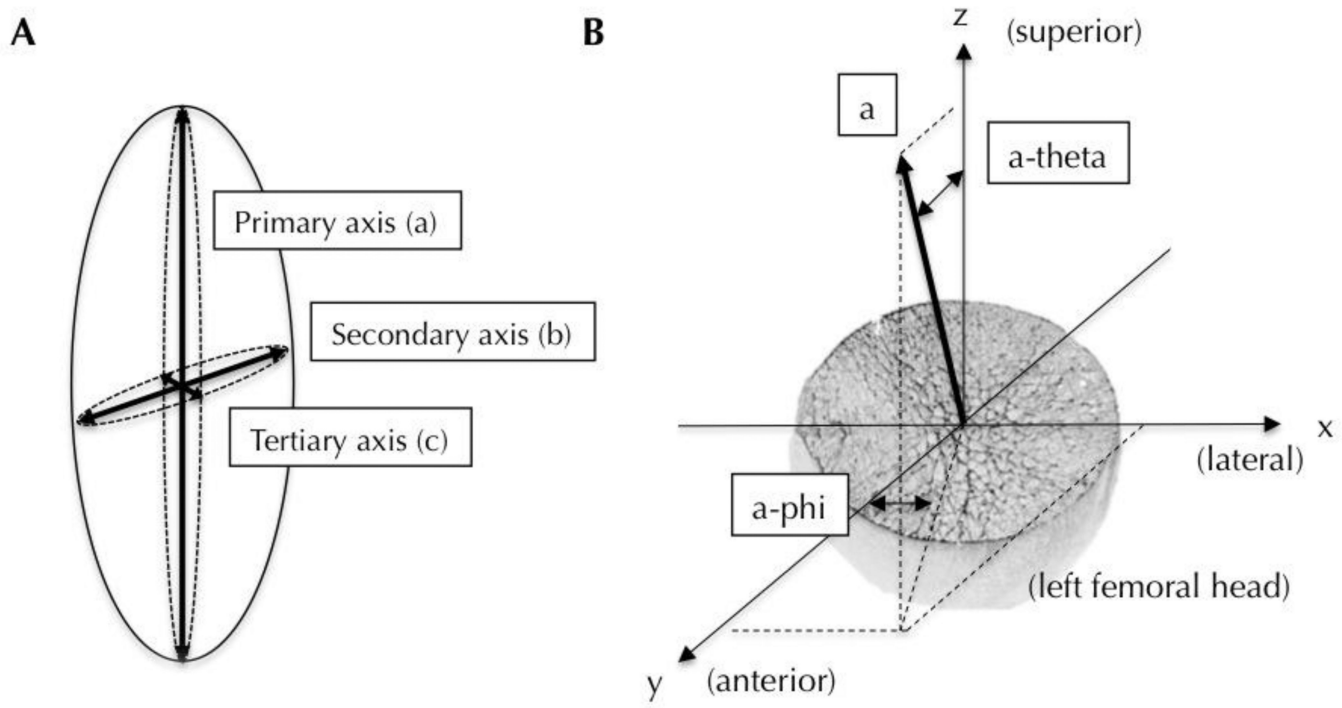

Fig. 3.

A–B, Anisotropy was calculated by the MIL method. Degree of anisotropy was defined as the length of the primary axis / tertiary axis of the MIL ellipsoid (DA=a/c) (A). High DA indicates high anisotropy. Orientation of anisotropy was defined as the absolute angle between the MIL axis, z-axis (theta) and y axis (phi) in this study (B). a-theta=0 means the bones are running supero-inferiorly, a-theta=90 indicates a horizontal orientation, a-phi=0 means the bones are running antero-posteriorly, and a-phi=90 means they run medio-laterally. In plate-like bones, b-theta and b-phi also define the orientation of the plate structure.

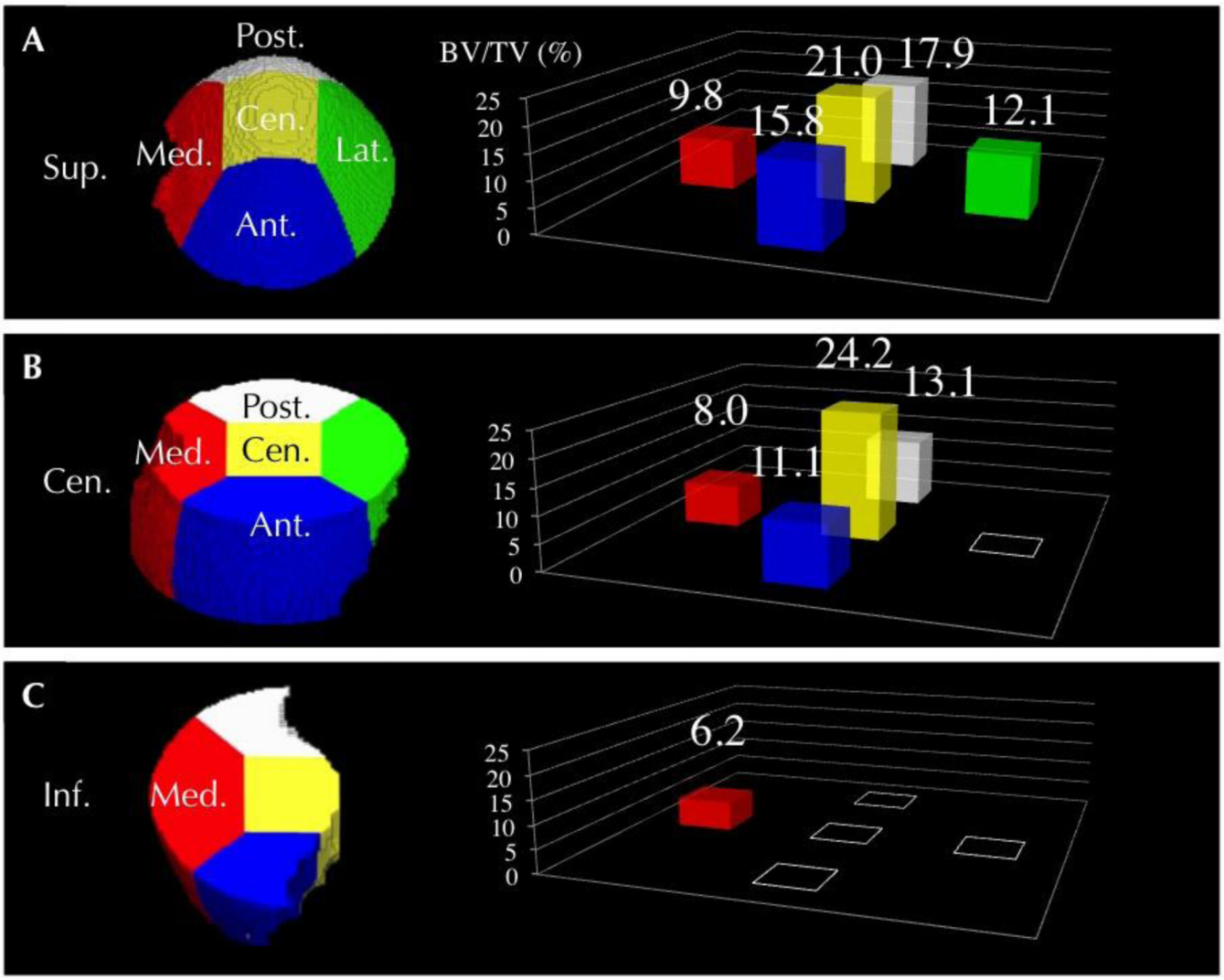

Fig. 4.

A–C, Regional distribution of BV/TV. BV/TV was higher in Cen-Cen, Sup-Cen, and Sup-Post regions. These regions would be weight bearing sites during standing and hip flex-extension movements. BV/TV at Cen-Ant and Cen-Post regions, where fixation of the screw for correcting a hip fracture may occasionally be improperly inserted, was almost half of Cen-Cen region.

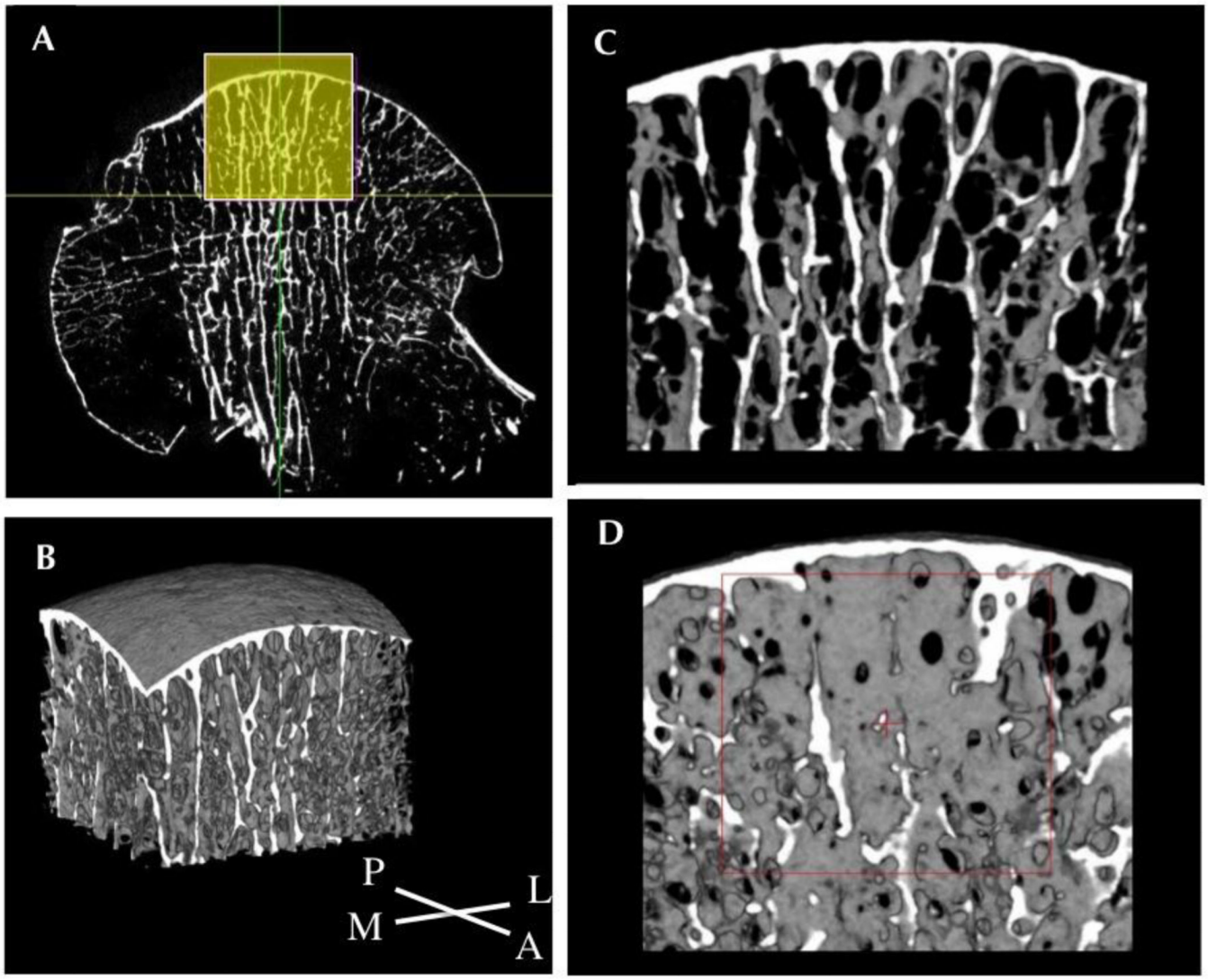

Fig. 5.

A–D, Features of trabecular bone structure at the Sup-Cen region (A and B: its orientation, C: AP view, D: Lat. view). Plate-like bone structure is predominantly observed in this region (SMI is average 1.59) and tend to run supero-inferiorly and antero-posteriorly (DA is 2.36, a-theta was 4.6, and b-phi was 9.3) (C, D). Weight bearing may indicate the need for the supero-inferior plate-like sturdy structure in this region. In addition, daily hip flex-extension movements (walk, sit down, stand up, etc.) might explain its antero-posterior orientation.

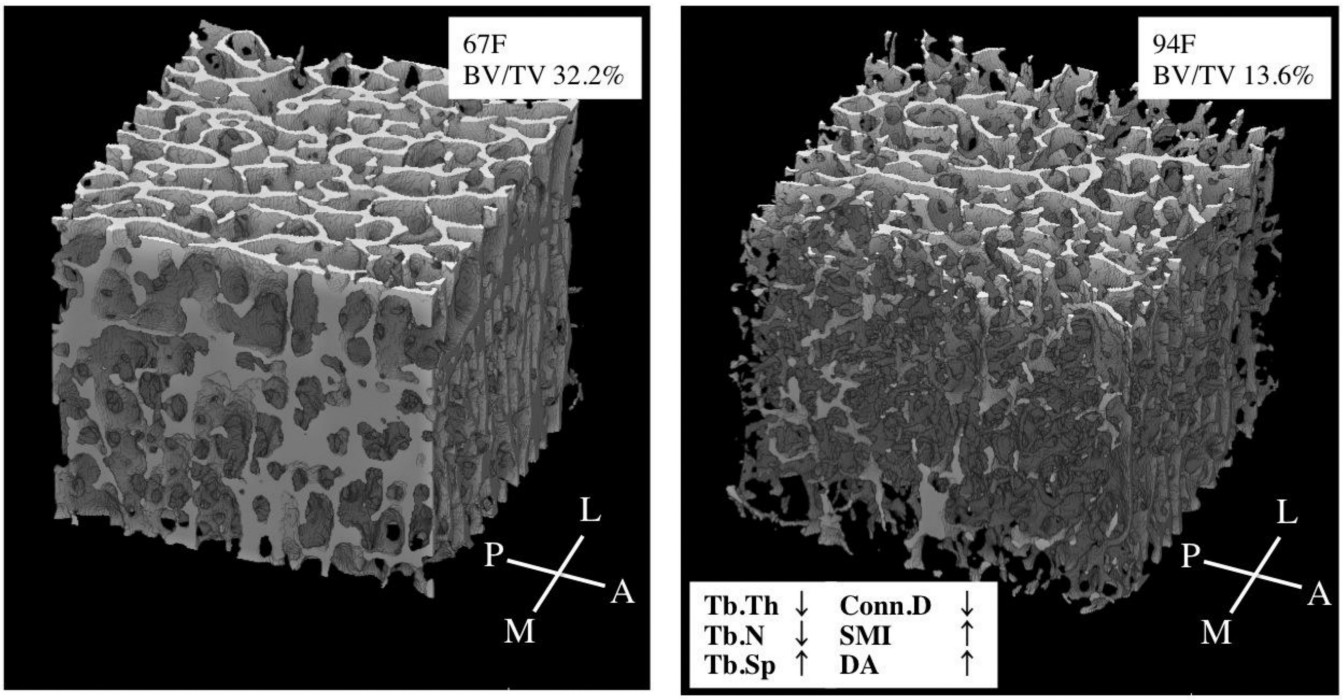

Fig. 6.

A–B, 3D images at the Cen-Cen region of 2 cases (BV/TV: 32.3 and 13.6 %). Lower BV/TV was related to lower Tb.Th, Tb.N, and Conn.D, and higher Tb.Sp, SMI (more rod-like structure), and DA. Due to OP progression and consistent with loss of bone connectivity, the plate-like structures became more rod-like. An increase in anisotropy may be explained by the loss of horizontal bone connectivity while vertical bone, which is more influence by weight bearing, remains relatively stable.

Table 1

Bone microstructural parameters in each region (Metric parameters)

Region	N	BV/TV (%)	Tb.Th (um)	Tb.N (/mm)	Tb.Sp (um)
Sup-Cen (SC)	15	21.0 ± 5.8(10.7–31.3) * (SM,SL,CM,CA,CP,IM)	239 ± 23 (198–277) * (CM,CP)	0.669 ± 0.121 (0454–0.889) * (SM,SL,CM,CA,IM)	708 ± 132 (563–924) * (IM)
Sup-Med (SM)	15	9.8 ± B6 (2.5–27.5) * (SC,SP,CC)	205 ± 37 (161–298) * (CC)	0.351 ± 0.157 (0.123–0.684) * (SC,SA,SP,CC)	857 ± 172 (618–1161) * (SP,CC)
Sup-Lat (SL)	15	12.1 ± 5.5 (4.1–25.4) * (SC,CC)	203 ± 19 (171–234) * (CC)	0.436 ± 0.156 (0.174–0.737) * (SC,SP,CC,IM)	772 ± 163 (509–1082) * (IM)
Sup-Ant (SA)	15	15.8 ± 6.1 (7.7–26.1) * (CC,CM,IM)	222 ± 18 (201–257) * (CC)	0.551 ± 0.153 (0.331–0.785) * (SM,CM,IM)	732 ± 160 (531–941) * (IM)
Sup-Pos (SP)	15	17.9 ± 6.4 (7.9–29.5) * (SM,CM,IM)	209 ± 20 (171–233) * (CC)	0.628 ± 0.138 (0.393–0.857) * (SM,SL,CM,CA,IM)	665 ± 120 (481–859) * (SM,CM,IM)
Cen-Cen (CC)	15	24.2 ± 5.6 (13.6–32.2) * (SM,SL,SA,CM,CA,CP,IM)	261 ± 29 (211–328) * (SM,SL,SA,CC,CM,CA,CP,IM)	0.676 ± 0.092 (0.571–0.812) * (SM,SL,CM,CA,IM)	667 ± 96 (526–819) * (SM,CM,IM)
Cen-Med (CM)	15	8.0 ± 4.0 (3.0–16.4) * (SC,SA,SP,CC)	190 ± 25 (160–235) * (SC,CC)	0.326 ± 0.102 (0.159–0.533) * (SC,SA,SP,CC,CP)	865 ± 139 (669–1095) * (SP,CC)
Cen-Ant (CA)	15	11.1 ± 4.1 (5.9–18.8) * (SC,CC)	216 ± 24 (194–283) * (CC)	0.413 ± 0.124 (0.258–0.632) * (SC,SP,CC)	845 ± 104 (710–1025)
Cen-Pos (CP)	14	13.1 ± 4.6 (6.3–20.8) * (SC,CC)	198 ± 20 (167–234) * (SC,CC)	0.527 ± 0.116 (0.334–0.735) * (CM,IM)	734 ± 84 (616–912) * (IM)
Inf-Med (IM)	12	6.2 ± 3.0 (2.9–11.8) * (SC,SA,SP,CC)	202 ± 55 (163–365) * (CC)	0.245 ± 0.074 (0.1 33–0.404) * (SC,SL,SA,SP,CC,CP)	980 ± 159 (694–1279) * (SC,SL,SA,SP,CC,CP)

BV/TV: bone volume fraction, Tb.Th: trabecular thickness, Tb.N: trabecular number. Tb.Sp: trabecular separation

(SC)-(IM) correspond each region, Values are average, standard deviation, minimum, and maximum

* Bonferroni test P<0.01, (underline); significantly higher, (*italy*): significantly lower

Table 2

Bone microstructural parameters in each region (Non-metric parameters)

Region	Conn.D (/mm^3)	SMI	DA	Primary Axis		Secondary Axis	
				|a-theta|	|a-phi|	|b-theta|	|b-phi|
Sup-Cen (SC)	1.86 ± 0.68 * (SM,CM,IM)	1.59 ± 0.33 * (SM,SL,SA,CM,CA,CP,IM)	2.36 ± 0.29 * (SM,SL,SA,CM,CA,CP,IM)	4.6 ± 2.0 †	46.1 ± 22.2	86.7 ± 2.2 ††††	9.3 ± 76
Sup-Med (SM)	0.73 ± 0.62 * (SC,SP,CC)	2.57 ± 0.39 * (SC,SP,CC)	1.64 ± 0.19 * (SC,SP,CC,CM)	34.2 ± 16.7	28 8 ± 27 7	58.6 ± 19.0	10.8 ± 7 1
Sup-Lat (SL)	1.19 ± 0 87	2.39 ± 0.34 * (SC,CC)	1.68 ± 0.20 * (SC,CC,CM)	23.9 ± 5.1	74.6 ± 11.7	74.7 ± 8.9	34.2 ± 27.1
Sup-Ant (SA)	1.45 ± 0.86 * (IM)	2.20 ± 0.32 * (SC,CC)	1.90 ± 0.24 * (SC,CC,CM,IM)	29.0 ± 5.4 ††	7.3 ± 4.7	61.8 ± 5.9 †††	10.3 ± 7.6
Sup-Pos (SP)	2.05 ± 1.08 * (SM,CM,CA,IM)	1.94 ± 0.37 * (SC,CM,CA,IM,CC)	1.96 ± 0.21 * (SC,CC, SM,CM,IM)	32.7 ± 7.4 †††	8.4 ± 5.3	57.7 ± 7.5 ††	13.5 ± 8 0
Cen-Cen (CC)	1.82 ± 0.39 * (SM,CM,IM)	1.33 ± 0.35 * (SM,SL,SA,SP,CM,CA,CP,CM)	2.34 ± 0.26 * (SM,SL,SA,SP,CM,CA,CP,IM)	4.4 ± 2.5 †	34.5 ± 17.4	86.3 ± 2.7 ††††	10.1 ± 7.1
Cen-Med (CM)	0.75 ± 0.49 * (SC,SP,CC)	2.54 ± 0.31 * (SC,SP,CC)	1.31 ± 0.13 * (SC,SM,SL,SA,SP,CC,CA,CP)	74.4 ± 19.9	47.0 ± 21.7	55.9 ± 28.7	37.3 ± 21.6
Cen-Ant (CA)	0.95 ± 0.50 * (SP)	2.40 ± 0.29 * (SC,SP,CC)	1.67 ± 0.16 * (SC,CC,CM)	37.2 ± 14.2 ††	9.1 ± 6.4	53.6 ± 14.4 †††	12.0 ± 9.1
Cen-Pos (CP)	1.49 ± 0.69 * (IM)	2.16 ± 0.34 * (SC,CC)	1.88 ± 0.15 * (SC,CC,CM,IM)	39.6 ± 12.7 †††	13.2 ± 8.3	50.6 ± 12.7 ††	15.8 ± 10.5
Inf-Med (IM)	0.43 ± 0.24 * (SC,SA,SP,CC,CP)	2.63 ± 0.19 * (SC,SP,CC)	1.48 ± 0.25 * (SC,SA,SP,CC,CP)	51.2 ± 31.1	62.7 ± 13.7	61.7 ± 21.2	46.6 ± 21.3

ConnD: connectivity density, SMI: structure model index, DA: degree of anisotrapy

|a-theta|: absolute angle between MIL primary axis and z (supero-inferior) axis, |a-phi|: absolute angle between MIL primary axis and y(antero-posterior) axis

|b-theta|: absolute angle between MIL secondary axis and z (supero-inferior) axis. |b-phi|: absolute angle between MIL secondary axis and y(antero-posterior) axis

(SC)-(IM) correspond each region, Values are average and standard deviation

* Bonferroni test P<0.01, (underline): significantly higher, (*italy*), significantly lower

† superior to inferior,

†† supero-anterior to infero-posterior,

††† supero-posterior to infero-anterior,

†††† anterior to posterior direction

Table 3

Correlation coefficient between BV/TV and the other microstructural parameters in each region

	Tb.Th	Tb.N	Tb.Sp	Conn.D	SMI	DA
Sup-Cen	0.81 *	0.87 *	−0.82 *	0.76 *	−0.92 *	−0.67 *
Sup-Med	0.84 *	0.89 *	−0.74 *	0.92 *	−0.97 *	0.33
Sup-Lat	0.69 *	0.91 *	−0.86 *	0.97 *	−0.94 *	−0.43
Sup-Ant	0.72 *	0.93 *	−0.87 *	0.94 *	−0.96 *	−0.70 *
Sup-Pos	0.75 *	0.98 *	−0.92 *	0.91 *	−0.96 *	−0.64 *
Cen-Cen	0.77 *	0.78 *	−0.84 *	0.76 *	−0.96 *	−0.80 *
Cen-Med	0.88 *	0.90 *	−0.72 *	0.98 *	−0.95 *	−0.10
Cen-Ant	0.60	0.91 *	−0.77 *	0.96 *	−0.94 *	−0.39
Cen-Pos	0.84 *	0.95 *	−0.80 *	0.96 *	−0.94 *	−0.34
Inf-Med	0.80 *	0.76 *	−0.69	0.85 *	−0.62	0.36

Tb.Th: trabecular thickness, Tb.N: trabecular number, Tb.Sp: trabecular separation

ConnD: connectivity density, SMI: structure model index, DA: degree of anisotropy

* Pearson's correlation test $p<0.01$